International Journal of Adhesion & Adhesives 33 (2012) 36–44

Contents lists available at SciVerse ScienceDirect

International Journal of Adhesion & Adhesives

journal homepage: www.elsevier.com/locate/ijadhadh

Limiting shear creep of epoxy adhesive at the FRP–concrete interface using multi-walled carbon nanotubes

Eslam Soliman [a], Usama F. Kandil [b], Mahmoud Reda Taha [a,*]

[a] Department of Civil Engineering, 1 University of New Mexico, MSC01 1070, NM 87131-0001, USA
[b] Egyptian Petroleum Research Institute, 1 Ahmed El-Zomor Street, Nasr City, Cairo 11727, Egypt

ARTICLE INFO

Article history:
Accepted 24 September 2011
Available online 25 October 2011

Keywords:
Interfaces
Rheology
Creep
Carbon nanotubes

ABSTRACT

Fiber reinforced polymer (FRP) composites are widely used in structural strengthening and retrofitting due to their high strength-to-weight ratio and non-corrosive properties. However, one of the recently recognized drawbacks of common FRP strengthening systems is the relatively high shear creep deformation of epoxy adhesives when FRP sheets are used to strengthen concrete structures against sustained loads. On the other hand, carbon nanotubes (CNTs) are reported to provide significant enhancement to various mechanical properties when used in epoxy adhesives. This enhancement is attributed to the extraordinary mechanical properties of the CNTs and their ability to bond to epoxy. In this article, we report the results of experimental and analytical investigations conducted to examine shear creep behavior of multi-walled carbon nanotubes (MWCNTs) reinforced epoxy nanocomposite used at the FRP–concrete interface. Double shear tests were performed on FRP sheets bonded to concrete blocks with MWCNTs reinforced epoxy nanocomposite. Various levels of pristine and functionalized MWCNTs by weight were examined including 0.1%, 0.5%, 1.0% and 1.5%. The viscoelastic behavior of MWCNTs reinforced epoxy nanocomposite was simulated with rheological models and the models' parameters were extracted and discussed. The results show the ability of MWCNTs to significantly reduce creep compliance of epoxy at the FRP–concrete interface making it a viable solution if FRP is used to strengthen concrete structures subjected to sustained stress.

1. Introduction

Retrofitting and strengthening of existing reinforced or prestressed concrete structures has been a rapidly growing area in civil engineering during the last few decades. Research efforts have focused on developing new techniques for strengthening because of two reasons (1) infrastructures designed in the 1950s–70s are now experiencing serious deterioration due to aging in harsh environments and (2) the development of various design codes to allow higher load-carrying capacities requires increasing the strength of existing structures even if they are functional. An excellent technique developed over the years is strengthening with fiber reinforced polymer (FRP) composites due to their high strength-to-weight ratio and durability. Researchers and designers have reported many field applications where FRP was used successfully in new structures [1] or in strengthening of existing structures [2]. However, on some occasions, this technique can experience premature failure and eventually lead to debonding due to the lack of shear transfer at the FRP–concrete interface. Furthermore, viscoelastic behavior (e.g. creep) of adhesives at the interface has been reported to be problematic when FRP strengthening was used to support sustained loads.

Recent experiments on full scale beams by Reda Taha et al. showed that creep of the epoxy adhesive was evident under sustained stress and can result in off-loading the FRP strips and thus cause later cracking of concrete [3]. The double lap shear test, proposed by the Japanese Concrete Institute, was used by Ferrier and Hamelin to examine the creep behavior of the FRP–concrete interface as a function of time and temperature and to estimate the parameters of the corresponding rheological models [4]. Feng et al. studied the creep behavior of structural adhesives by means of accelerated creep tests [5]. It was found that long-term creep behavior of epoxy adhesives can be reliably predicted from a set of short-term accelerated creep tests. Benyoucef et al. developed a closed form solution to describe shear creep and shrinkage of adhesives at the FRP–concrete interface [6]. From their theoretical approach, reduction of interfacial stress was predicted as the thickness of the adhesive increased. It was also observed by Wu and Diab that creep of adhesives significantly increases the bond length of the FRP [7]. Meshgin et al. used the double shear test to examine the effects of different parameters on the creep response of epoxy at the FRP–concrete interface [8]. The epoxy thickness, curing time and shear

* Corresponding author. Tel.: +505 277 1258; fax: +505 277 1988.
E-mail address: mrtaha@unm.edu (M. Reda Taha).

0143-7496/$ - see front matter © 2011 Elsevier Ltd. All rights reserved.
doi:10.1016/j.ijadhadh.2011.09.006

stress level were found to significantly affect the shear creep compliance. In addition, Majda and Skrodzewich [9] examined the effects of the stress level on the creep of epoxy adhesive under tension and developed rheological models. They showed that stress level has significant impact on the values of the parameters in the rheological models. Furthermore, Hamed and Bradford [10] found that creep results in significant shear and normal stresses of the adhesives at its edges. Recently, Ferrier et al. [11] examined the time–temperature correspondence of epoxy adhesives having different glass-transition (T_g) temperatures subjected to shear loading and concluded that creep is strongly correlated to the T_g of epoxy.

Since their discovery by Iijima [12], carbon nanotubes (CNTs) have been the research focus of many scientists worldwide as they investigate CNTs' properties and develop techniques to increase their production capacities. Currently, applications of CNTs include polymer, metal and ceramic matrix composites, scanning probe tips, and contact devices for nano electro mechanical systems (NEMS) devices [13]. A great deal of effort has been spent on CNTs research due to their outstanding mechanical, electrical and thermal properties. CNTs are known to have mechanical properties one or more order of magnitude greater than all conventional structural materials. For example, Young's modulus of CNTs is 10–100 times higher than the strongest steel [14]. A large area of CNTs research focuses on their use with polymers to produce nanocomposites. Much of the research on CNTs in polymer matrices has addressed two drawbacks that interfere with enhancing the mechanical response: difficulty in dispersing CNTs in the matrix and poor interfacial bond between CNTs and the matrix. Various techniques have been developed to overcome these challenges such as surfactant treatment [15–17] and functionalization [18–20].

The time dependant behavior of CNTs-polymer nanocomposites is rarely examined. Suhr et al. examined the viscoelastic behavior of thin epoxy film with multi-walled carbon nanotubes (MWCNTs) under shear and observed 1400% increase in damping ratio [21]. Moreover, Zhang et al. investigated the creep behavior of CNTs reinforced epoxy nanocomposite under tension and observed reduction in creep strain up to 30% with 0.1% single-walled carbon nanotubes (SWCNTs) [22]. Significant enhancement in creep resistance of magnetically oriented CNTs reinforced epoxy nanocomposite was also observed by Tehrani and Al-Haik [23].

It is noted that the creep behavior of adhesives at the FRP–concrete interface has been recently investigated and characterized during the last decade. A good understanding of the mechanics and behavior of epoxy at FRP–concrete interface has been developed [3–10]. However, few or no studies are directed to improve the shear creep behavior of these adhesives. The objective of this study is to use CNTs to reduce the long-term creep deformations of epoxy adhesive at the FRP–concrete interface subjected to sustained loads. Improving the shear creep behavior of the adhesive used with FRP composites would be beneficial to existing strengthening systems. To examine the MWCNTS reinforced epoxy bondlines, double lap shear tests were performed on FRP–concrete joints. Rheological models are developed to predict the experimental results and to understand the role of CNTs in limiting creep of epoxy adhesive at the FRP–concrete interface. In addition, the rheological model can be used with the finite element method to simulate shear creep behavior of adhesive in modeling reinforced concrete (RC) elements strengthened with FRP strips.

2. Experimental methods

The double lap shear test was used to evaluate creep of epoxy with CNTs at the FRP-concrete interface. The double lap shear test specimen consisted of two carbon fiber reinforced polymer (CFRP) composite strips bonded to two sides of two concrete blocks with controlled thickness epoxy adhesive as shown in Fig. 1. The concrete blocks were loaded in tension to induce shear stresses at the four epoxy joints. The applied load (P) induced shear stress of 25% of the shear strength of the epoxy. DEMEC (strain gage) points were bonded to the concrete blocks and used to measure the deformation of two shear joints in the loading direction. Creep deformation of FRP itself was minimized by choosing unidirectional CFRP strips and orienting the fiber direction parallel to the direction of the applied load. In addition, the axial stress in concrete during experiments did not exceed 0.36 MPa (less than 10% of the tensile strength of concrete). Therefore, creep and shrinkage of concrete during the experiment was expected to be negligible compared with epoxy creep. By neglecting creep and shrinkage of concrete and creep of the CFRP strips and ignoring the deformation through epoxy thickness, epoxy shear strain $\gamma(t)$

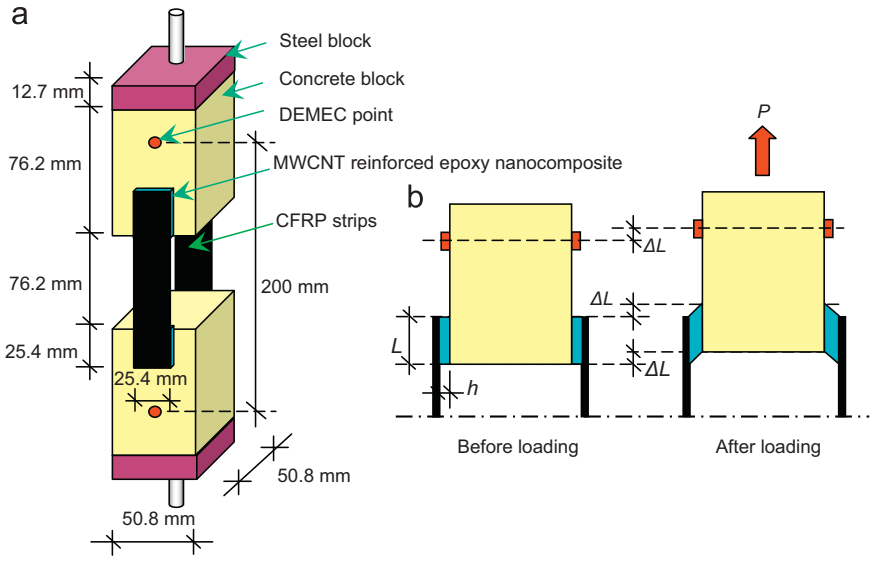

Fig. 1. Schematic of the double lap shear specimen (a) dimensions and (b) deformation.

per joint can be computed as

$$\gamma(t) = \Delta L(t)/h \quad (1)$$

where h is the epoxy thickness, t is the time and $\Delta L(t)$ is the shear displacement per joint and is obtained by measuring the change in the distance between the two DEMEC points due to the applied sustained load. In addition, the shear stress τ acting on every shear joint can be computed as

$$\tau = P/2A \quad (2)$$

where A is the area of one shear joint. The normalized creep compliance $J_n(t)$ of epoxy is also computed relative to the elastic deformation from the following equation:

$$J_n(t) = \gamma(t)/[\tau J(0)] \quad (3)$$

where $J(0)$ is the elastic compliance and $\gamma(t)/\tau$ is the creep compliance.

2.1. Materials

Concrete mix (360 kg Portland cement, 90 kg class (F) fly ash, 150 l of water and 1729 kg of aggregate with 1:1 fine to coarse aggregate) is used as substrates for all experiments. The chosen concrete mix has a 28-day compressive strength of 42 MPa, similar to most concrete used nowadays in construction of reinforced or prestressed concrete elements. The CNTs were supplied by Cheap Tubes, Inc. Based on the manufacturer's specifications, the CNTs are multi-walled (MWCNTs) with outer diameter (OD) of 20–30 nm, inner diameter (ID) of 5–10 nm and length of 10–30 μm with an aspect ratio of 500–1000. The bulk density of the MWCNTs is 0.21 g/cm^3 and the specific surface area is 110 m^2/gm. The nanotubes are manufactured by catalytic chemical vapor deposition (CCVD) technique with purity being greater than 95% by weight. Two types of MWCNTs were supplied and used, pristine (with no chemical treatment) and functionalized, with carboxyl groups (COOH). The functionalized MWCNTs had functional groups of 1.23% by weight.

The epoxy used in fabrication is EPOTUF® 37–127, a liquid resin epoxy system supplied by U.S. Composites, Inc. The epoxy resin is low viscosity, 100% reactive diluted liquid based on Bisphenol-A, containing glycidyl ether (DGEBPA). The hardener is aliphatic amine EPOTUF® 37–614. The resin to hardener mixing ratio is 2:1, the pot life is 30–45 min at 26.7 °C and the setting time is 5–6 h, with a drying time of 24–28 h. The tensile strength and elongation at break are 68.9 MPa and 2.5%, respectively. The resin viscosity at room temperature is 600 cps. The low viscosity of the resin facilitates incorporating the MWCNTs during the fabrication process and provides reasonable levels of deformations in order to obtain accurate creep measurements. The CFRP composites were supplied by Graphtek LLC Company. The CFRPs were 1.1 mm thick uni-directional strips fabricated with 33-msi carbon and Vinlester resin. Density, tensile strength and flexural strength of the CFRP laminates were 1.49 g/cm^3, 2689 MPa and 1875.4 MPa, respectively.

2.2. MWCNTs dispersion in epoxy nanocomposite

One of the major challenges of incorporating MWCNTs in polymers is to obtain a uniform dispersion of the MWCNTs. The difficulty of dispersing the MWCNTs in the matrix is due to the van der Waals forces between the MWCNTs, which promotes entanglement of the MWCNTs with each other. Over the last decade, several techniques were developed to obtain homogeneously dispersed MWCNTs in the polymer suspension and to avoid the formation of MWCNTs agglomerations such as surfactant treatment or functionalization. The functionalization helps in dispersing the nanotubes due to negative or positive charges of the functional groups that counteract the van der Waals forces. It also increases the interfacial bond between the nanotubes and the surrounding polymer chains. In this study, both pristine and functionalized MWCNTs are examined.

Three different types of treated epoxies were produced to fabricate the epoxy adhesive bondlines in this study. The first type was neat epoxy prepared by mixing the resin (component A) with the hardener (component B) and applying the mixture directly at the CFRP–concrete interface to form the bondline. The second type was prepared by reinforcing the epoxy with pristine MWCNTs and is referred to as (P). The dispersion was performed by adding the required MWCNTs content to the epoxy resin (component A) only and the MWCNTs–resin mixture was sonicated in an ultrasonic bath for 1.0 h at 40 °C. The reason for heating the resin is to decrease the resin's viscosity, which helps in dispersing the nanotubes. The hardener (component B) was added afterward to the MWCNTs–resin dispersion. The third type was prepared by reinforcing the epoxy with functionalized COOH-MWCNTs and is referred to as (F). The functionalized MWCNTs were added first to the resin (component A) with 1.0 h sonication at 40 °C. In order to ensure chemical interaction between the functional groups on the surface of the nanotubes and the resin chains, the dispersed mixture was stirred for 2.0 h at 80 °C. The hardener (component B) was added after cooling the resin and the MWCNTs reinforced epoxy nanocomposite was ready to use.

2.3. Bondlines fabrication and testing methods

In order to examine the creep of the FRP–concrete interface, nine double lap shear specimens were fabricated and tested under sustained loads. The first specimen was fabricated with neat epoxy without MWCNTs (first type). Four other specimens were fabricated with pristine MWCNTS reinforced epoxy nanocomposite with various pristine MWCNTs loadings (second type). The various loadings of the pristine MWCNTs by weight of epoxy were 0.1%, 0.5%, 1.0% and 1.5%. In the last four specimens, the functionalized MWCNTS reinforced epoxy nanocomposites were used with the same four loadings of MWCNTs (third type). In addition to the creep specimens, similar specimens with neat epoxy were fabricated and tested to failure to obtain the bond strength of the shear joint.

$50.8 \times 50.8 \times 76.2$ mm concrete blocks were cast and cured in a water bath for one week. After wet curing, the concrete was left to dry for three weeks. $50.8 \times 50.8 \times 12.5$ mm steel blocks were bonded to the ends of the concrete blocks. The adhesives between the steel and concrete blocks were left to cure for a week. The prepared MWCNTS reinforced epoxy nanocomposites were cast on 25.4×25.4 mm shear joint. Class VI soda-lime glass beads, 0.71 ± 0.035 mm diameter, supplied by Mo-Sci Corporation were used to control the epoxy thickness following the recommendations of ASTM D5868-01 [24] for lap shear test. The glass beads were added to the concrete surface in an amount equivalent to 0.5% by volume of epoxy. After this, the epoxy was injected by syringe pump onto the surface of the concrete. A pressure of 34 kPa was applied by steel weights after placing the CFRP strips over the epoxy shear joint and any excess epoxy was carefully removed. This procedure minimized the formation of air bubbles in the bondlines. The shear joint was cured for 14 day at room temperature before applying the sustained load. The shear strength test was performed with MTS® Bionix servo hydraulic system (Fig. 2). Two strength tests were performed on neat epoxy: double lap shear test with the epoxy at the CFRP–concrete and single lap shear test with the epoxy at the CFRP–CFRP interface. Both specimens were loaded to failure by displacement controlled mode at a loading rate of 0.5 mm/min.

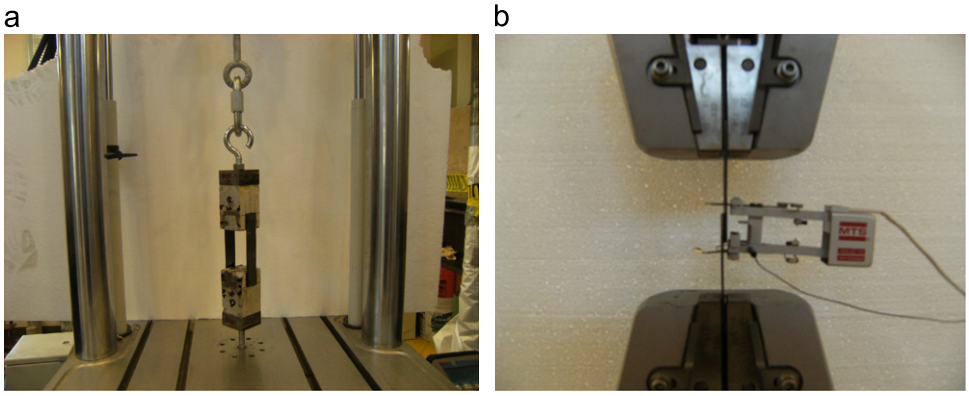

Fig. 2. Shear strength test performed on epoxy bondlines: (a) test setup for double lap shear specimen and (b) test setup for single lap shear specimen.

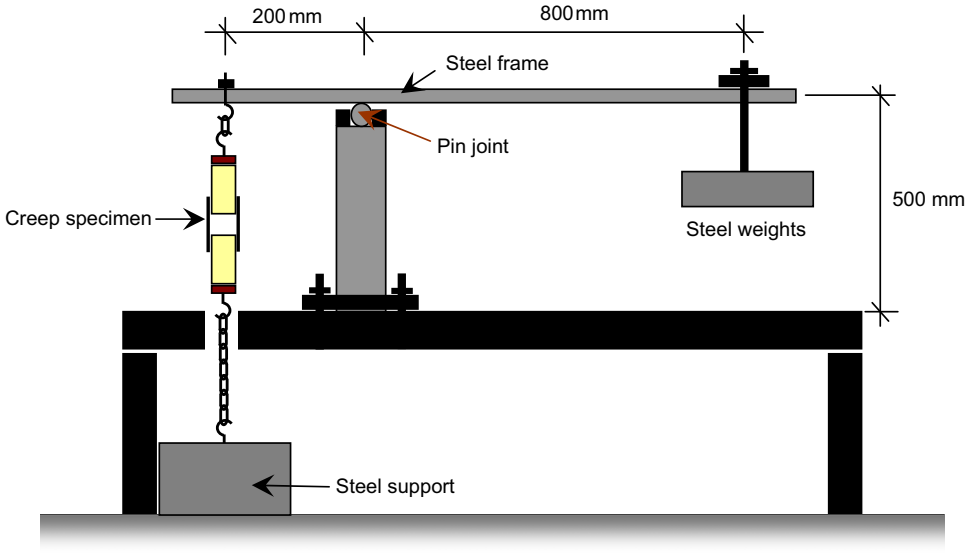

Fig. 3. Schematic of creep test setup.

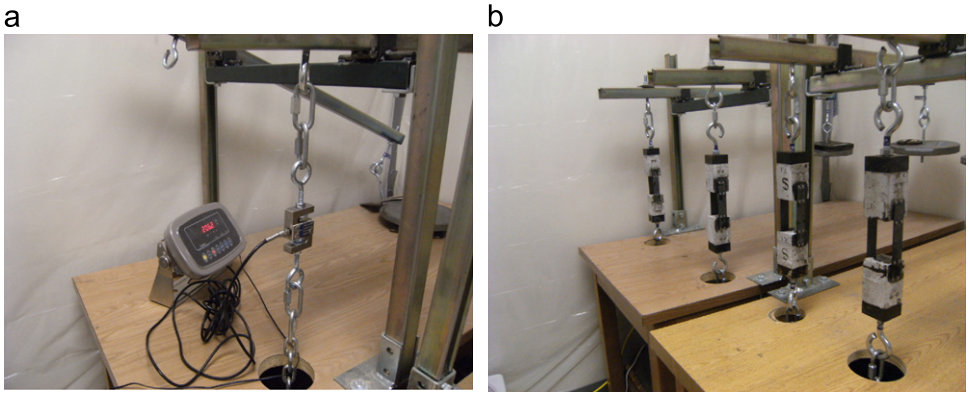

Fig. 4. Creep experiment performed on four specimens: (a) load cell attached to determine creep load and (b) four creep specimens loaded.

DEMEC strain gauges supplied by Mayes Instruments, Ltd. were installed by means of a reference bar and dial gage and were used to obtain strain measurements during the creep experiment. The specimens were then loaded in a creep loading frame (Fig. 3). The applied load was measured with load cell (Fig. 4(a)) and a load level of 934 ± 22 N was maintained at the specimen. This load level induced shear stress of 724 ± 17 kPa at each shear joint, which corresponds to 25% of the shear strength. A system of steel hooks and chains were used in transferring the load to the double shear specimens to avoid inducing any eccentricities. The creep experiments were performed under a controlled environment of relative humidity (RH) of 40% and temperature of 23 °C. Temperature variation effects are not considered to be a critical parameter in epoxies used at FRP–concrete interfaces in civil infrastructure. Fig. 4(b) shows the four creep specimens attached to the loading frames.

3. Rheological modeling

Rheological models have been widely used to simulate the behavior of viscoelastic materials such as polymer, concrete and masonry due to their simplicity and practicality. They provide a tool for understanding the physical phenomena including the instantaneous and time-dependant deformations. In addition, the modularity of rheological models allows development of different models by means of different arrangements and combinations of springs and dashpots. During the last decade, many researchers have used rheological models to describe epoxy adhesives' behavior at the FRP–concrete interface [4,7,8,11]. In this study, the effect of incorporating MWCNTs into epoxy adhesives is considered. Several rheological models are considered and all but two are ruled out. The effect of MWCNTs is included implicitly in the parameters of the model.

Fig. 5 shows some basic rheological models developed to describe the behavior of viscoelastic materials. Maxwell (Fig. 5(a)) and Kelvin (Fig. 5(b)) are two-parameter models, which consist of springs and dashpots connected in series and parallel, respectively. The two-parameter models are inefficient in predicting the creep behavior of adhesives because of their lack of simulating some basic phenomena. For example, the Maxwell model fails in simulating a decreased creep strain rate under constant stress while the Kelvin model fails in simulating the instantaneous deformations [25]. On the other hand, four-parameter models such as Burgers (Fig. 5(g)) are abundant in describing the creep behavior of polymers. Three-parameter models such as Ross (Fig. 5(c)), Modified Maxwell (MM) (Fig. 5(d)), and other models (Fig. 5(e) and (f)) have a sufficient number of parameters to predict the behavior. Models Fig. 5(e) and (f) can be excluded because of their lack of instantaneous deformation. Therefore, two models are considered in this study, Ross (Fig. 5(c)) and Modified Maxwell (MM) (Fig. 5(d)) models. The long-term strain $\varepsilon(t)$ under sustained stress σ_0 for the two models can be described as follows:

$$\varepsilon(t)=\frac{\sigma_0}{R_1}+\frac{\sigma_0}{R_2}\left[1-\exp\left(\frac{-tR_2}{\mu_2}\right)\right] \quad \text{for Ross model} \tag{4}$$

$$\varepsilon(t)=\frac{\sigma_0}{R_2}-\left(\frac{\sigma_0}{R_2}-\varepsilon_0\right)\exp\left[\frac{-t}{\mu_1(1+(R_2/R_1))}\right] \quad \text{for MM model} \tag{5}$$

where R_1 and R_2 are the elastic moduli coefficients, ε_0 is the instantaneous strain and μ_1 and μ_2 are the viscosity coefficients. Given the strain formula and by following similar procedures as in Section 2.1, the normalized creep compliances are computed as follows ([25], Appendix A):

$$J_n(t)=\frac{1}{\varepsilon_0}\left[\frac{\sigma_0}{R_1}+\frac{\sigma_0}{R_2}\left(1-\exp\left[\frac{-tR_2}{\mu_2}\right]\right)\right] \quad \text{for Ross model} \tag{6}$$

$$J_n(t)=\frac{1}{\varepsilon_0}\left[\frac{\sigma_0}{R_2}-\left(\frac{\sigma_0}{R_2}-\varepsilon_0\right)\exp\left(\frac{-t}{\mu_1(1+(R_2/R_1))}\right)\right] \quad \text{for MM model} \tag{7}$$

In addition, Ross and MM models are evaluated by computing the root mean square prediction error *RMSE* between the predicted and the experimental data

$$RMSE=\sqrt{\sum_{i=1}^{N}\frac{(J_{ni}^{\exp}-J_{ni}^{\text{pred}})^2}{N}} \tag{8}$$

where N is the number of creep data points, $J_{ni}^{\exp}$ is the normalized creep compliance for the ith experimental data point and J_{ni}^{pred} is the normalized creep compliance for the ith predicted data point. It

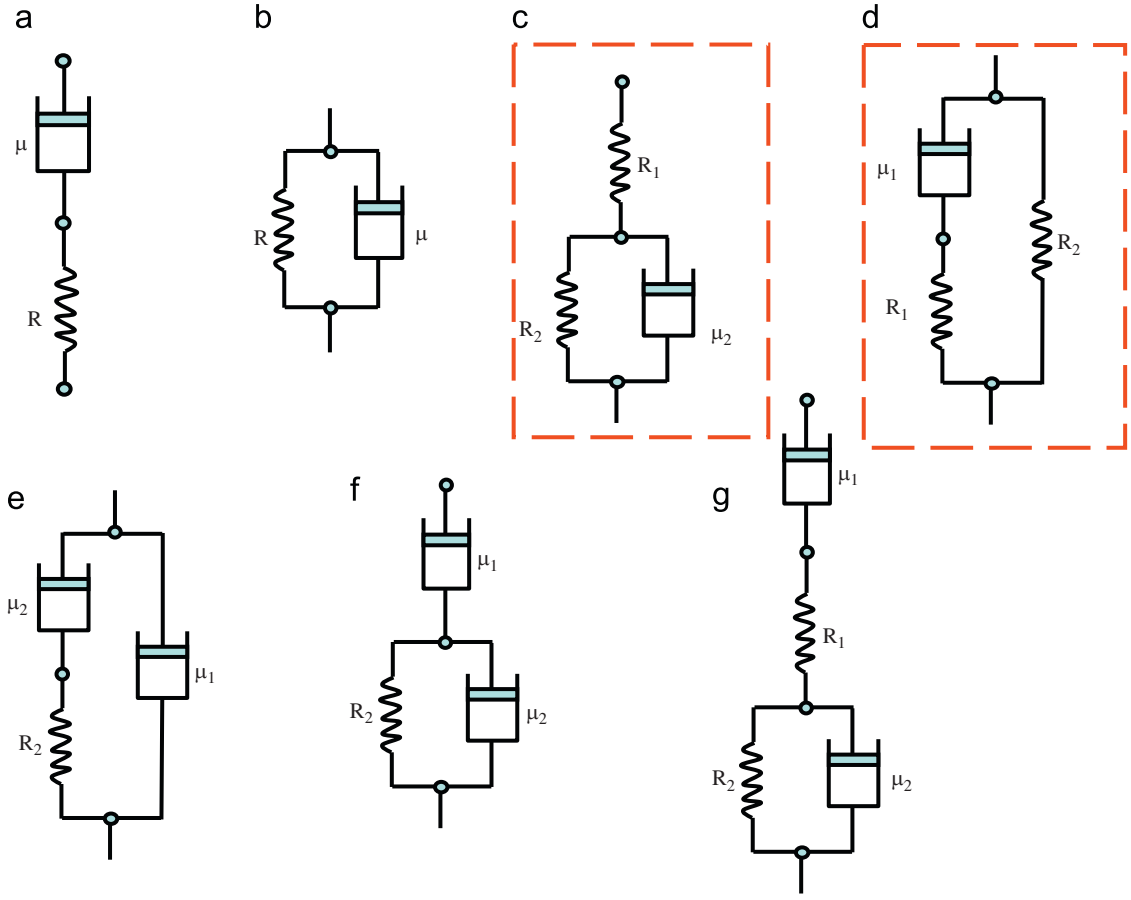

Fig. 5. Various combinations of rheological models with (a–b) two parameters (c–f) three parameters and (g) four parameters.

is important to note that the classical Ross and MM models might be able to simulate creep behavior of neat epoxy, but they cannot represent the significance of MWCNTs on creep of epoxy. Therefore, in order to represent the significance of MWCNTs loadings, we suggest modifying both models to account for the MWCNTs loading $\alpha =$ (weight of CNTs/weight of epoxy). The new Ross and MM models are denoted as MWCNT-Ross and MWCNT-MM, respectively. In these models, the elastic moduli coefficients R_1 and R_2 as well as the viscosity coefficients μ_1 and μ_2 are presented as a function of the MWCNTs loading α.

4. Results and discussion

4.1. Experimental results

Fig. 6 shows the failure of lap shear joints. The double lap shear test (Fig. 6(a)) exhibited shear failure in the concrete substrate. Therefore, the strength obtained from the double shear test represents the concrete shear strength rather than the epoxy bond strength. On the other hand, the single lap shear test (Fig. 6(b)), in which the failure occurred at the CFRP–CFRP interface, provided accurate estimation of the shear strength of the epoxy adhesive at the FRP interface. The estimated shear strengths from the double and single lap shear joints based on the same interfacial area (645.16 mm^2) are 2521 and 2822 kPa, respectively. A choice was made afterwards to apply sustained shear stress equal to 25% of the bond strength.

Elastic shear strains of 0.17%, 0.12%, 0.11%, 0.20% and 0.21% were exhibited by neat epoxy, 0.1%, 0.5%, 1.0% and 1.5% pristine MWCNTS reinforced epoxy nanocomposites, respectively. This observation demonstrates that the highest elastic shear modulus was obtained in the case of 0.5% pristine MWCNTs while the lowest was obtained in the 1.5% pristine MWCNTs. In the case of functionalized MWCNTs, the elastic shear strains were 0.18%, 0.10%, 0.12% and 0.13% for MWCNTs contents of 0.1%, 0.5%, 1.0% and 1.5%, respectively. The average elastic shear strain in the case of functionalized MWCNTs (0.1325%) was less than that of the pristine MWCNTs (0.160%), which indicates higher elastic shear modulus in the functionalized case. As in the pristine case, the 0.5% functionalized MWCNTs case exhibited the highest shear modulus. Moreover, the maximum shear strains after 1 month of creep under the sustained load were 0.87%, 0.72%, 0.57%, 1.04% and 1.03% for pristine MWCNTS contents of 0%, 0.1%, 0.5%, 1.0% and 1.5%, respectively. The shear strains corresponding to functionalized MWCNTS contents of 0.1%, 0.5%, 1.0% and 1.5% were 0.42%, 0.39%, 0.38% and 0.35%, respectively. The shear strains show that the functionalized MWCNTs reduced the creep strain of the epoxy adhesive at the interface significantly.

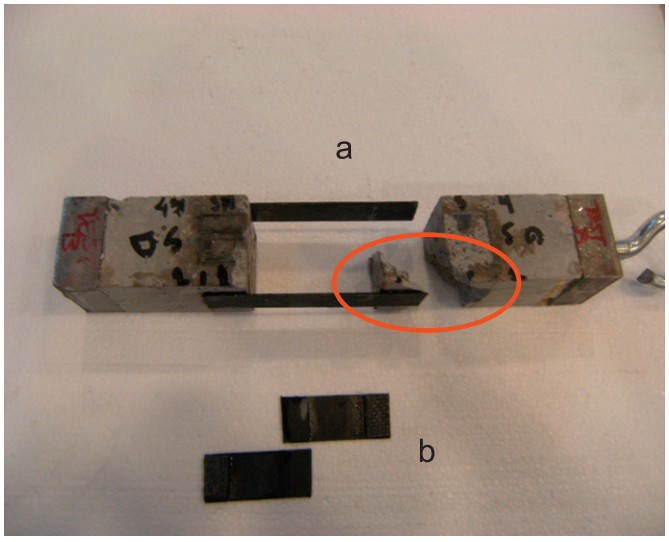

Fig. 6. Failure of lap shear joints: (a) double lap and (b) single lap.

The normalized creep compliances J_n were computed and plotted with time in Fig. 7(a) and (b) for the pristine and functionalized MWCNTS reinforced epoxy nanocomposites. In general, it can be noted from Fig. 7(a) and (b) that the addition of pristine MWCNTs had limited effect on the normalized creep compliance of MWCNTS reinforced epoxy nanocomposite. On the other hand, the functionalized MWCNTs reduced the creep compliance significantly. The case of 0.1% functionalized MWCNTs had the largest decrease in creep compliance among all cases and the creep compliance was reduced by 54% with respect to the neat epoxy. This is attributed to the fact that with low loadings of MWCNTs, it is easier to disperse MWCNTs in the epoxy matrix. Thus, it is easier to obtain a uniform microstructure. As the MWCNTs content increases, difficulties in dispersion arise due to the formation of MWCNTs agglomerations. The interfacial bond between the epoxy and the MWCNTs seems to be a critical parameter in long-term shear creep deformation of epoxy adhesives at the FRP–concrete interfaces since the functionalized MWCNTs significantly outperformed the pristine MWCNTs (Fig. 8). The average increase in normalized creep compliance with pristine MWCNTs was 8% while the average decrease was 40% with functionalized MWCNTs. It is evident from the experiments that shear creep of epoxy at the FRP–concrete interface under sustained loads can be significantly limited by incorporating functionalized MWCNTs.

4.2. Rheological modeling

Since there was no significant effect of pristine MWCNTs on the creep behavior of epoxy, only the specimens with functionalized MWCNTs reinforced epoxy nanocomposite were simulated with rheological models. Figs. 9 and 10 depict MWCNT-Ross and MWCNT-MM rheological models fitting curves for various functionalized MWCNTs loadings. As shown in the figures, the two models are capable of predicting creep compliance of MWCNTs reinforced epoxy nanocomposite with small *RMSE*. The relatively small *RMSE* values for the two models indicate that three parameters are sufficient in describing the shear creep behavior of functionalized MWCNTS reinforced epoxy nanocomposite at the FRP–concrete interface. The average *RMSEs* for the MWCNT-Ross and MWCNT-MM models were 0.094 and 0.111, respectively. This indicates that MWCNT-Ross model slightly outperformed MWCNT-MM model in predicting shear creep behavior of epoxy at the FRP–concrete interface when functionalized MWCNTSs are incorporated.

Figs. 11 and 12 show the effect of various functionalized MWCNTs loadings on MWCNT-Ross and MWCNT-MM models, respectively. The elastic moduli for the springs in Figs. 11(a) and 12(a) for the two models increased with the addition of the functionalized MWCNTs. However, the shape of the increase differs from each elastic modulus and each model. For instance, the elastic moduli R_1 and R_2 for MWCNT-Ross model varies with the functionalized MWCNTs content according to third-order polynomial functions as shown in Eqs. (9) and (10). On the other hand, the elastic modulus R_1 for MWCNT-MM varies according to second order polynomial function (Eq. (11)). Moreover, by separating the neat epoxy ($\alpha = 0$) data point, it can be noticed that the elastic modulus R_2 varies linearly with the MWCNTs content (Eq. (12)).

MWCNT-Ross model

$$R_1 = 639.3(\alpha)^3 - 1737.9(\alpha)^2 + 1287.6(\alpha) + 294.8 \text{ in MPa} \quad (9)$$

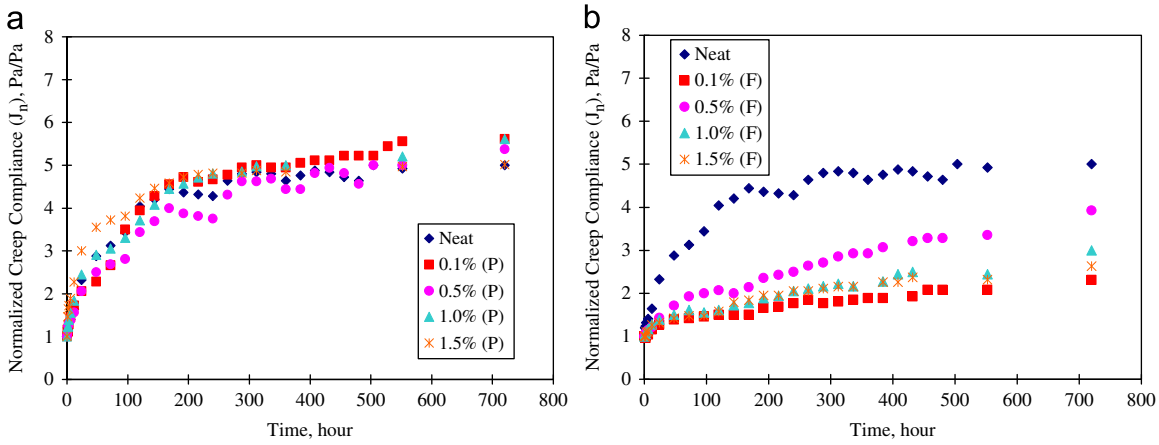

Fig. 7. Normalized creep compliance of FRP–concrete interface with various MWCNTs loadings: (a) pristine and (b) functionalized.

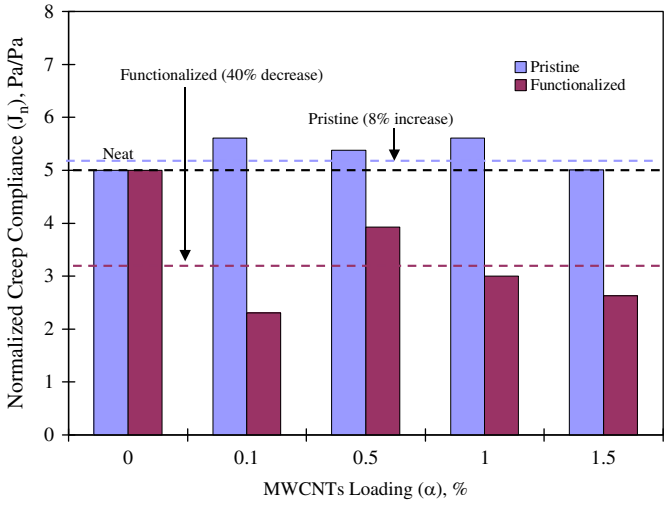

Fig. 8. Comparison between the pristine and functionalized MWCNTs in terms of normalized creep compliance.

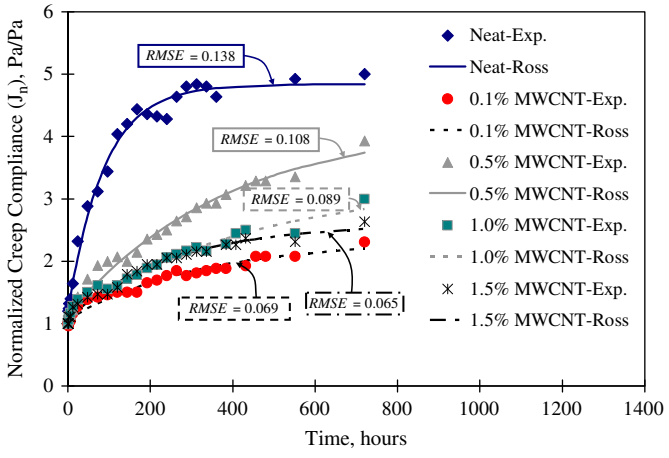

Fig. 9. Fitting of normalized creep compliance data for functionalized MWCNTs with Ross model and MWCNT-Ross model.

$$R_2 = 599.2(\alpha)^3 - 1579.1(\alpha)^2 + 1075.8(\alpha) + 144.4 \text{ in MPa} \quad (10)$$

MWCNT-MM model

$$R_1 = 135.5(\alpha)^2 - 209.3(\alpha) + 174.3 \text{ in MPa} \quad (11)$$

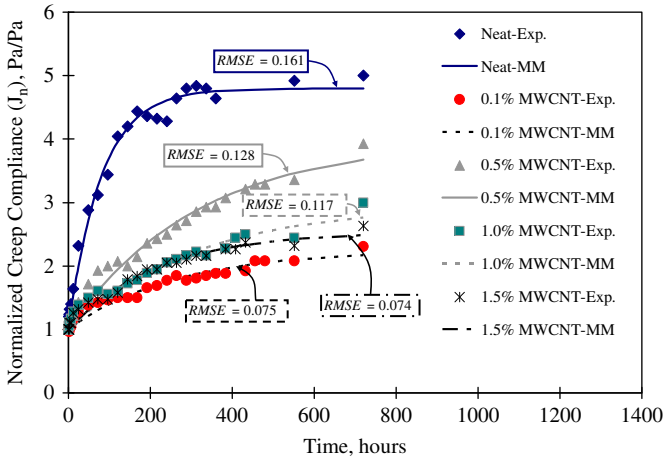

Fig. 10. Fitting of normalized creep compliance data for functionalized MWCNTs with Modified Maxwell (MM) model and MWCNT-MM model.

$$\begin{cases} R_2 = 80 \text{ in MPa } E\ \alpha \le 0.1 \\ R_2 = 23.95(\alpha) + 162.3 \text{ in MPa for } \alpha > 0.1 \end{cases} \quad (12)$$

More emphasis is placed on studying the effect of adding functionalized MWCNTs on the viscosity coefficients μ_1 and μ_2 for the dashpot due to their importance on the viscous and long-term behavior of epoxy. In the case of MWCNT-Ross model, the coefficient of viscosity increased on average by 900% due to adding functionalized MWCNTs, while 200% average increase was observed in the case of MWCNT-MM model (Figs. 11(b) and 12(b)). The viscosity coefficients μ_1 and μ_2 also varied with the loading, α, of the functionalized MWCNTs in the epoxy. Eqs. (13) and (14) describe the relation as second- and third-order polynomials for the MWCNT-Ross and MWCNT-MM models, respectively. From these results, it is obvious that the effect of functionalized MWCNTs on creep of epoxy at the FRP–concrete interfaces can be modeled by means of rheological models. These established relationships between the rheological model parameters and the MWCNTs loading α are useful for numerical analysis of FRP–concrete interface.

MWCNT-Ross model

$$\mu_2 = -99.4(\alpha)^2 + 180.5(\alpha) + 35.5 \text{ in GPa.sec} \quad (13)$$

MWCNT-MM model

$$\mu_1 = 168.5(\alpha)^3 - 467.3(\alpha)^2 + 345.7(\alpha) + 63.4 \text{ in MPa.sec} \quad (14)$$

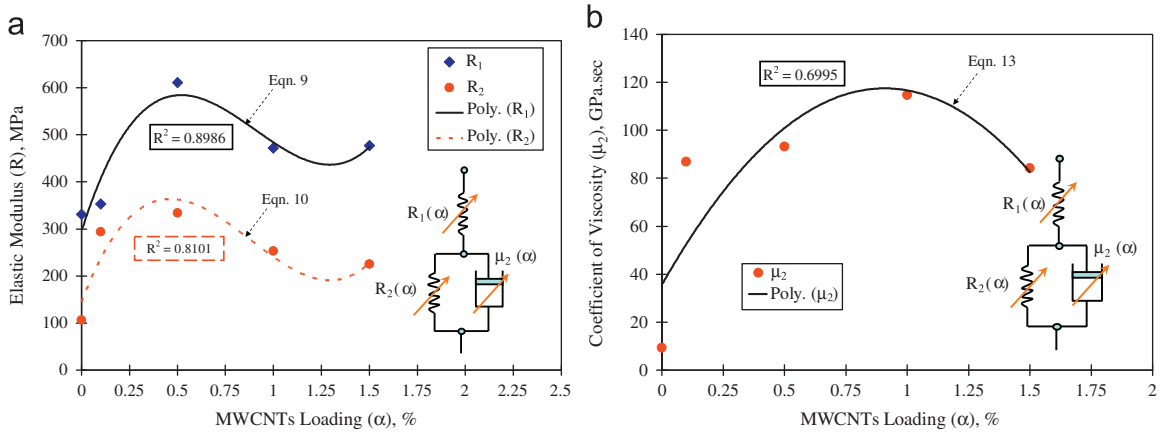

Fig. 11. Effect of MWCNTs on MWCNT-Ross model parameters: (a) elastic moduli and (b) viscosity coefficient.

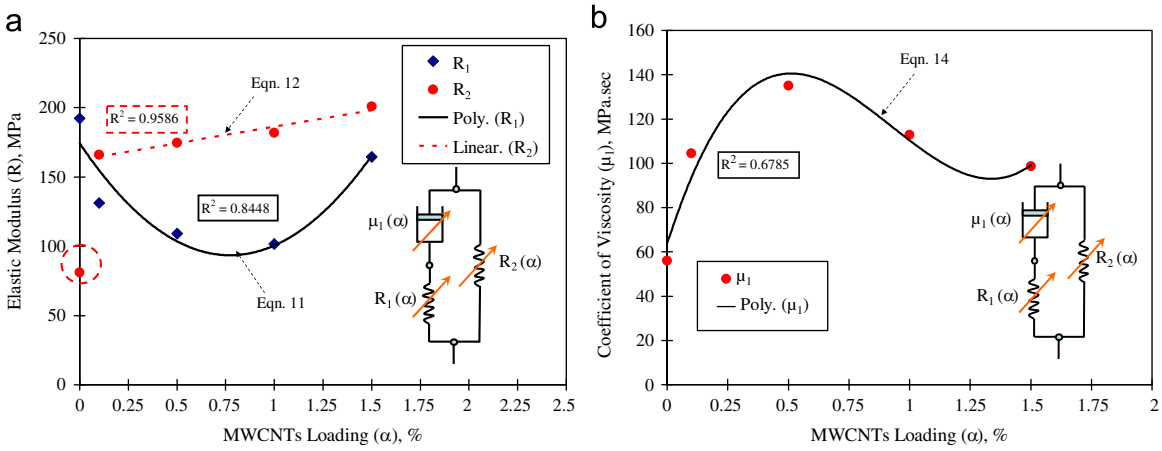

Fig. 12. Effect of MWCNTs on MWCNT-MM model parameters: (a) elastic moduli and (b) viscosity coefficient.

Finally, it is worth noting that an early 2011 quick market survey showed that with the use of large amount of MWCNTs in the production of epoxy adhesives, in the order of metric tons, the price of MWCNTs will have a limited impact on total composite cost. For instance, the cost of adding 0.1–1.0% MWCNTs functionalized MWCNTs to epoxy represents a cost increase of 20–30% of the current epoxy cost. This is believed to be a very small cost given the pronounced effect of functionalized MWCNTs on limiting the creep of epoxy adhesives at the FRP–concrete interface.

5. Conclusions

Creep experiments of FRP–epoxy–concrete interfaces were performed on double lap shear test specimens. The effect of incorporating various contents of pristine and functionalized MWCNTs on creep of epoxy at the concrete–FRP interface is investigated. In general, little to no effect is observed with the use of pristine MWCNTs. However, functionalized MWCNTs were able to limit shear creep of epoxy significantly. The use of functionalized MWCNTs at the 0.1% level (per weight of epoxy) out-performed all other MWCNTs loadings and resulted in 54% reduction in normalized creep compliance. These observations indicate the importance of chemical functionalization of MWCNTs in reducing shear creep strains of epoxy nanocomposite. In addition, the effect of the functionalized MWCNTs on the creep of adhesives is simulated by rheological modeling. Two modified rheological models are suggested to simulate creep behavior of MWCNTS reinforced epoxy nanocomposite. The functionalized MWCNTs increased the viscosity coefficients significantly. The effect of MWCNTs as described by the suggested models agrees well with experimental results. These rheological models would be beneficial for simulating creep behavior of epoxy in numerical models for FRP–concrete interface under sustained loads.

Acknowledgements

The authors greatly acknowledge funding by Defense Threat Reduction Agency (DTRA) Grant # HDTRA1-08-1–0017 P00001. Funding to the second author by Science and Technology Development Fund (STDF) for US–Egypt Junior Researcher Program is greatly appreciated. Recent funding by NSF US-Egypt Cooperative Research program to the authors Award # 1103601 is also acknowledged.

Appendix A

In Fig. A.1, from strain compatibility, the total strain can be computed as

$$\varepsilon(t) = \varepsilon_{R_2} = \varepsilon_{\mu_1} + \varepsilon_{R_1} \quad \text{(A.1)}$$

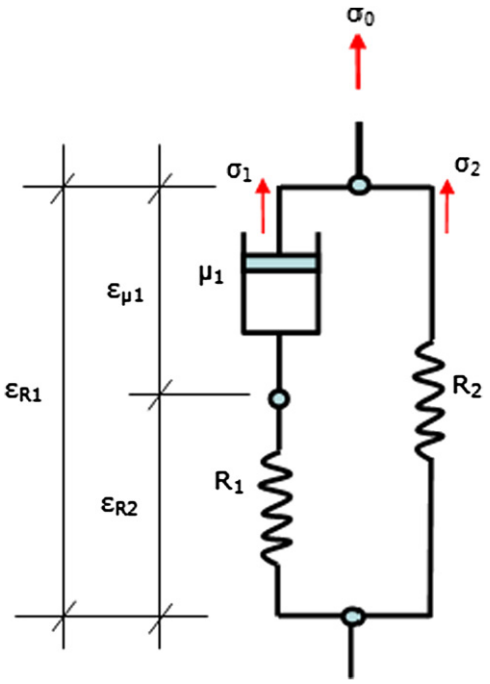

Fig. A1. Modified Maxwell model for predicting creep.

By differentiating Eq. (A.1) with respect to time and considering spring and dashpot relations results in

$$\frac{\partial\varepsilon(t)}{\partial t}=\frac{1}{R_1}\frac{\partial\sigma_1(t)}{\partial t}+\frac{\sigma_1(t)}{\mu_1} \tag{A.2}$$

From stress equilibrium $\sigma_0=\sigma_1(t)+\sigma_2(t)$ results in

$$\frac{\partial}{\partial t}[\varepsilon(t)]=\frac{1}{R_1}\frac{\partial\sigma_0}{\partial t}-\frac{1}{R_1}\frac{\partial[\sigma_2(t)]}{\partial t}+\frac{\sigma_0-\sigma_2(t)}{\mu_1} \tag{A.3}$$

Since constant stress condition and spring Hooke's law imply $\partial\sigma_0/\partial t=0$ and $\sigma_2(t)=R_2\varepsilon(t)$ then

$$\int\frac{d\varepsilon(t)}{\sigma_0-R_2\varepsilon(t)}=\int\frac{dt}{\mu_1(1+(R_2/R_1))} \tag{A.4}$$

By integrating Eq. (A.4), the total strain becomes

$$\varepsilon(t)=\frac{\sigma}{R_2}-\exp\left(\frac{-t}{\mu_1(1+(R_2/R_1))}+C\right) \tag{A.5}$$

Considering the initial conditions $t=0\Rightarrow\varepsilon(t)=\varepsilon_0$

$$C=\ln\left(\frac{\sigma}{R_2}-\varepsilon_0\right)\ \text{ and }\ \varepsilon(t)=\frac{\sigma_0}{R_2}-\left(\frac{\sigma_0}{R_2}-\varepsilon_0\right)\exp\left(\frac{-t}{\mu_1(1+(R_2/R_1))}\right) \tag{A.6}$$

Since the total compliance is $J(t)=\varepsilon(t)/\sigma_0$, the elastic compliance is $J(0)=\varepsilon_0/\sigma_0$, and the normalized creep compliance is $J_n(t)=J(t)/J(0)$, the normalized creep compliance becomes

$$J_n(t)=\frac{1}{\varepsilon_0}\left[\frac{\sigma_0}{R_2}-\left(\frac{\sigma_0}{R_2}-\varepsilon_0\right)\exp\left(\frac{-t}{\mu_1(1+(R_2/R_1))}\right)\right] \tag{A.7}$$

References

[1] Nanni A. FRP reinforcement for bridge structures. In: Proceedings of the structural engineering conference. Lawrence, KS: The University of Kansas; 2000.
[2] Reda Taha M, Tromposch E, Tadros G, Mufti A, Klowak C. Performance based design for FRP strengthening of the roof panels of Calgary Saddledome, vol. 215. American Concrete Institute, SP; 2003 (pp. 385–398).
[3] Reda Taha MM, Masia MJ, Choi K-K, Shrive PL, Shrive NG. Creep effects in plain and FRP-strengthened RC beams. ACI Struct J 2010;107:627–35.
[4] Ferrier E, Hamelin P. Long-term concrete–composite interface characterization for reliability prediction of RC beam strengthened with FRP. Mater Struct 2002;35:564–72.
[5] Feng CW, Keong CW, Hsueh YP, Wang YY, Sue HJ. Modeling of long-term creep behavior of structural epoxy adhesives. Int J Adhes Adhes 2005;25:427–36.
[6] Benyoucef S, Tounsi A, Adda Bedia EA, Meftah SA. Creep and shrinkage effect on adhesive stresses in RC beams strengthened with composite laminates. Compos Sci Technol 2007;67:933–42.
[7] Wu Z, Diab H. Constitutive model for time-dependent behavior of FRP–concrete interface. J Compos Constr ASCE 2007;11:477–86.
[8] Meshgin P, Choi K, Reda Taha MM. Experimental and analytical investigations of creep of epoxy adhesive at the concrete–FRP interfaces. Int J Adhes Adhes 2009;29:56–66.
[9] Majda P, Skrodzewicz J. A modified creep model of epoxy adhesive at ambient temperature. Int J Adhes Adhes 2009;29:369–404.
[10] Hamed E, Bradford MA. Creep in concrete beams strengthened with composite materials. Eur J Mech A/Solids 2010;29:951–65.
[11] Ferrier E, Michel L, Jurkiewiez B, Hamelin P. Creep behavior of adhesives used for external FRP strengthening of RC structures. Constr Build Mater 2011;25:461–7.
[12] Iijima S. Helical microtubules of graphitic carbon. Nature 1991;354:56–8.
[13] Eklund P, Ajayan P, Blackmon R, Hart AJ, Kong J, Pradhan B, et al. International assessment of carbon nanotube manufacturing and applications. Final Report. World Technology Evaluation Center, Inc.; 2007.
[14] Advani SG, Fan Z. Dispersion, bonding and orientation of carbon nanotubes in polymer matrices. Processing and properties of nanocomposites. World Scientific Publishing Company Pte. Ltd.; 2007 [Chapter 2].
[15] Gong X, Liu J, Baskaran S, Voise RD, Young JS. Surfactant-assisted processing of carbon nanotube/polymer composites. Chem Mater 2000;12:1049–52.
[16] Islam MF, Rojas E, Bergey DM, Johnson AT, Yodh AG. High weight fraction surfactant solubilization of single-wall carbon nanotubes in water. Nano Lett 2003;3:269–73.
[17] Geng Y, Liu MY, Li J, Shi XM, Kim JK. Effects of surfactant treatment on mechanical and electrical properties of CNT/epoxy nanocomposites. Compos Part A 2008;39:1876–83.
[18] Zhu J, Kim JD, Peng H, Margrave JL, Khabashesku VN, Barrera EV. Improving the dispersion and integration of single-walled carbon nanotubes in epoxy composites through functionalization. Nano Lett 2003;3:1107–13.
[19] Breton Y, Desarmot G, Salvetat JP, Delpeux S, Sinturel C, Beguin F, et al. Mechanical properties of MWNT/epoxy composites: influence of network morphology. Carbon 2004;42:1027–30.
[20] Gojny FH, Wichmann M, Fiedler B, Schulte K. Influence of different carbon nanotubes on the mechanical properties of epoxy matrix composites—a comparative study. Compos Sci Technol 2005;65:2300–13.
[21] Suhr J, Koratkar N, Keblinski P, Ajayan P. Viscoelasticity in carbon nanotube composites. Nat Mater 2005;4:134–7.
[22] Zhang W, Joshi A, Wang Z, Kane RS, Koratkar N. Creep mitigation in composites using carbon nanotube additives. Nanotechnology 2007;18:1–5.
[23] Tehrani M, Al-Haik M. Magnetically enhanced mechanical and creep properties of a structural epoxy. Int J Mater Struct Integr 2009;3:147–60.
[24] ASTM D5868-01. Standard test method for lap shear adhesion for fiber reinforced plastic (FRP) bonding. PA: ASTM International; 2008.
[25] Findley WN, Lai JS, Onaran K. Creep and relaxation of nonlinear viscoelastic materials. New York: Dover Publications Inc.; 1989.